Interactions between propagating cracks and bioinspired self-healing vascules embedded in glass fibre reinforced composites

C.J. Norris, R.S. Trask, I.P. Bond

Interactions between propagating cracks and bioinspired self-healing vascules embedded in glass fibre reinforced composites

C.J. Norris, R.S. Trask, I.P. Bond

PII: S0266-3538(11)00055-8
DOI: 10.1016/j.compscitech.2011.01.027
Reference: CSTE 4922

To appear in: *Composites Science and Technology*

Received Date: 6 December 2010
Revised Date: 27 January 2011
Accepted Date: 30 January 2011

Please cite this article as: Norris, C.J., Trask, R.S., Bond, I.P., Interactions between propagating cracks and bioinspired self-healing vascules embedded in glass fibre reinforced composites, *Composites Science and Technology* (2011), doi: 10.1016/j.compscitech.2011.01.027

Interactions between propagating cracks and bioinspired self-healing vascules embedded in glass fibre reinforced composites

C.J. Norris, R.S. Trask*, I.P. Bond

Advanced Composites Centre for Innovation and Science (ACCIS), Department of Aerospace Engineering, University of Bristol, Queen's Buildings, University Walk, Bristol BS8 1TR, UK

Abstract

This study considers the embedment of a bioinspired vasculature within a composite structure that is capable of delivering functional agents from an external reservoir to regions of internal damage. Breach of the vascules, by propagating cracks, is a crucial pre-requisite for such a self-healing system to be activated. Two segregated vascule fabrication techniques are demonstrated, and their interactions with propagating Mode I and II cracks determined. The vascule fabrication route adopted played a significant role on the resulting laminate morphology which in-turn dictated the crack-vascule interactions. Embedment of the vascules did not lower the Mode I or II fracture toughness of the host laminate, with vascules orientated transverse to the crack propagation direction leading to significant increases in G_I and G_{II} through crack arrest. Large resin pockets were found to redirect the crack around the vascules under Mode II conditions, therefore, it is recommended to avoid this configuration for self-healing applications.

*Corresponding author. Tel: +44 (0) 1173315845; Fax: +44 (0) 1179545666; E-mail address: R.S.Trask@bristol.ac.uk

Keywords: Smart Materials (A), Fracture Toughness (B), Damage Tolerance (D), Self-healing.

1. Introduction

Under impact loading, a fibre reinforced epoxy polymer (FRP) dissipates energy through elastic deformation and damage formation mechanisms, as governed by the planar microstructure of the fibre reinforcement and the inherent brittleness of the epoxy matrix. Such damage formation can lead to significant reductions in mechanical performance whilst leaving little surface evidence of

the impact event; a situation termed *barely visible impact damage* (BVID) [1-3]. Within the aerospace industry, the current structural design philosophy is to allow large margins to account for the potential reductions in mechanical performance from operationally induced damage. However, if the damage were autonomously healed by entities embedded within the composite component, then conservative designs could be avoided, leading to lighter more fuel efficient transport. Of course, the embedment of functional components should not impart a mass penalty of their own for this philosophy to hold [4]. At present, it should be recognised that composite structures are designed based on strength and stiffness criteria rather than being fracture mechanics driven. This study presents the first findings in support for a change to a damage tolerance design philosophy, through the utilisation of a self-healing microvascular network.

The incorporation of self-healing delivery systems within an FRP is an active area of research, aimed at mimicking the healing process found in the biological kingdom. This function has been imparted to an FRP laminate by the incorporation of filled compartmentalised vessels, in the form of microcapsules [5-7] or hollow glass fibres [8-10]. This approach is reliant on an impact event to fracture the vessels and 'bleed' the contained mobile liquid phase into the damaged region. The supply of healing agent is directly related to the number of vessels incorporated within the composite structure and will become depleted locally after the first damage event. Replenishment of healing agent is not viable, leaving the delivery system redundant and unable to heal subsequent damage events. Interconnected, pervasive vascular networks, akin to those

found in living organisms, have been embedded in bulk polymeric materials [11,12] and the core structures of composite sandwich panels [13,14]. In both cases a replenishable and repeated self-healing function was demonstrated. The host materials ability to form around the inclusion caused negligible knockdown in mechanical performance. To embed such a vasculature within an FRP laminate without disrupting the fibre architecture offers a significantly tougher challenge, one that is yet to be fully met.

Plantae-inspired, segregated vascules have been successfully created within a fibre-reinforced polymer composite laminate, via a lost wax process. Such vascules are capable of providing an ongoing self-healing function without incurring a mass penalty. Two fabrication routes have been demonstrated, with the vascule preform material either laid between plies [15-17] or nested in pre-cut recesses within the plies [18] during the stacking sequence. Regardless of the fabrication route utilised, it has been shown that the vascules should be aligned to both the local fibre direction and loading direction to avoid significant reductions in mechanical performance. The latter study showed that the vascule fabrication route and location in the ply stack played a significant role in determining the vascule-damage connectivity, a pre-requisite for effective self-healing.

Embedded vasculatures should be breached by a propagating crack, and not just rely on direct interaction with an impact event to initiate self-healing. The primary goal of the ongoing CRack Arrest and Self-Healing in Composite Structures (CRASHCOMPS) project is to manipulate cracks within composite structures such that they are directed to a region of self-healing. In conjunction,

these approaches provide the ability to arrest and heal critical cracks. From a self-healing viewpoint, it is imperative to understand how propagating cracks interact with embedded healing agent delivery systems. It has been shown that incorporation of open galleries within an FRP leads to significant arrest of Mode I propagating cracks, through a blunting mechanism [19], and the crack-gallery interactions were such that healing agent delivery could be expected. In this study, the interactions of propagating Mode I and II cracks with self-healing vasculature, aligned or transverse to the fibre direction, are investigated. Two fabrication routes are evaluated, the vascule preform material laid between plies (fabrication route A) or nested in pre-cut recesses within the ply stacking sequence (fabrication route B).

2. Manufacture and vascule characterisation

Unidirectional glass fibre reinforced epoxy (HexPly 913, Hexcel Composites) was selected due to its translucency, allowing easy monitoring of an internal crack front. A 28-ply unidirectional laminate (3.8mm nominal thickness) was chosen for the fracture toughness evaluations based on the ASTM guidelines for Mode I testing [20]. All laminates were cured to the manufacturer's recommendations, 125°C for 1 hr and a pressure of 700 kPa.

Steel wire with a diameter of 0.5mm, pre-coated with a PTFE release spray to ease removal post-cure, was selected as the vascule preform material. For fabrication route A, the vascule preform wires were located at the laminate mid-plane between the two central plies. To incorporate the steel wires via fabrication route B, the four central plies were cut at the desired vascule

location. Four plies were cut to create the recess necessary for 0.5mm wires based on the nominal ply thickness of the pre-impregnated tape (0.135mm, determined experimentally). The same techniques were used to prepare specimens containing vascules orientated parallel or transverse to the fibre orientation. It should be noted that, for fabrication route B, the fibres were terminated at the position of the ply cuts for transverse vascule orientation. In all cases a spacing of 10mm was maintained between the vascules. Following is a list of the vascule configurations evaluated, along with a nomenclature that will be used in the subsequent text:

- Transverse, fabrication route A = TA
- Transverse, fabrication route B = TB
- Parallel, fabrication route A = PA
- Parallel, fabrication route B = PB

The vascules were sectioned and inspected via optical microscopy (Olympus SZX16 microscope with ColorView camera), with typical micrographs of the laminate microstructures provided in **Fig. 1**. Embedding a vascule transverse to the fibre orientation, via fabrication route A, led to significant fibre waviness and the formation of large resin pockets, in-line with the findings of previous studies [15-19]. The corresponding vascule formed via fabrication route B shows the elimination of fibre waviness but resin pockets still persist at the corners of the square recess created during fabrication. Alignment of the vascule to the fibre direction eliminates fibre waviness and resin pockets as the fibres ‘fit’ around the wire during the laminate cure cycle. The effects of the

different vascule microstructures on the Mode I and II Interlaminar fracture toughness are discussed in the following sections.

3. Test methology

3.1 Mode I Double Cantilever Beam (DCB) testing

Testing was based on ASTM D5528-01 [20]. However, due to the translucency of the laminates, crack propagation was monitored via a video camera situated above the sample (**Fig. 2**), as opposed to the monitoring of crack growth with the aid of a visual enhancement on the sample edge. The samples were tested on an Instron 3343 with a 1kN load cell at a displacement rate of 2mm/ min, applied via piano hinges bonded to the specimens with Redux 810, **Fig. 3**. A PTFE crack initiator (15μm film thickness) was located on the laminate mid-plane, after which the crack propagation was allowed to stabilise over a 25mm length before meeting the first vascule. The cracks were propagated for a total of 100mm before stopping the test, with a minimum of five specimens tested for each vascule configuration. The mode I strain energy release rate (G_I) was calculated using the modified beam theory:

$$G_I = \frac{3P\delta}{2b(a+\Delta_I)} \qquad (1)$$

Where, P represents the applied load, δ the load point displacement, b the specimen thickness and a the delamination length. As the beam in not perfectly built-in, rotation may occur at the delamination front; therefore a correction factor Δ_I is incorporated which treats the DCB specimen as if it contained a slightly longer delamination. Δ_I was calculated experimentally by generating a

least squares plot of the cube root of compliance, $C^{1/3}$, as a function of delamination length [20].

3.2 Mode II End Loaded Split (ELS) testing

Stable Mode II propagating cracks have been successfully evaluated by numerous researchers using the ELS configuration, e.g. [21-23]. In the absence of a recognised standard, testing was based on the guidelines provided by the European Structural Integrity Society, Technical Committee 4 [24]. For ease of manufacture, the laminate dimensions were kept consistent with those used for Mode I, therefore, the specimen thickness was less than the recommended 5mm for glass FRP systems. Specimens were clamped in the ELS fixture and loaded to create a 5mm pre-crack prior to commencing the Mode II fracture toughness test. Crack propagation was monitored via a video camera situated above the sample, as for the DCB evaluations. Testing was carried out on an Instron 8872 with a 10kN load cell at a displacement rate of 2mm/ min. The specimen geometry for the Mode II ELS testing matched that used for the DCB testing, however, the load was applied to a section of aluminium T-bar bonded to the upper surface rather than using piano hinges, **Fig. 4**. The specimens were clamped in the ELS fixture to ensure $a/L \geq 0.55$ was satisfied for stable crack propagation [21,25] (where a is the crack length and L the free length of the specimen). This gave a crack propagation length of 45mm. A minimum of five specimens were tested for each vascule configuration.

The mode II strain energy release rate (G_{II}) was calculated using the corrected beam theory:

$$G_{II} = \frac{9P^2(a+\Delta_{II})^2}{4B^2Eh^3} \qquad (2)$$

Where, P represents the applied load, a the delamination length, Δ_{II} the delamination length correction ($\Delta_{II} = 0.42\ \Delta_I$), B the specimen width, E the flexural modulus (48 GPa as specified by the manufacturer) and h the half thickness of the specimen. Large displacements and load block corrections have to be applied, leading to a corrected value of G_{II}:

$$G_{II(corrected)} = G_{II}\left[1-\theta_1\left(\frac{\delta}{L}\right)^2-\theta_2\left(\frac{\delta l_1}{L^2}\right)\right] \qquad (3)$$

Where, l_1 is the distance from the centre of the load block to the mid-plane of the specimen and δ is the displacement. The correction factors θ_1 and θ_2 were obtained from:

$$\theta_1 = \frac{3}{20}\frac{\left[15+50\left(\frac{a}{L}\right)^2+63\left(\frac{a}{L}\right)^4\right]}{\left[1+3\left(\frac{a}{L}\right)^3\right]^2} \qquad (4)$$

$$\theta_2 = -3\left(\frac{L}{a}\right)\frac{\left[1+3\left(\frac{a}{L}\right)^2\right]}{\left[1+3\left(\frac{a}{L}\right)^3\right]} \qquad (5)$$

4. Results and discussion

4.1 Mode I crack-vascule interactions

Controlled crack propagation under Mode I opening displacement was easily achieved. Typical load-displacement curves for specimens containing vascules

transverse to the fibre direction, along with a control sample, are provided in **Fig. 5**. The crack propagation in the specimens containing vascules proceeded as for the control until approximately 2mm from the first vascule (experimental observation). At this point, the crack jumped into the vascule, resulting in a sharp load drop. The observations were consistent for both vascule formation routes and confirmed them to be successful Mode I crack attractors. This is expected for fabrication route A, where **Fig. 1(a)** clearly shows the resin pocket to extend at least 2mm from the edge of the vascule. However, the resin pockets produced during fabrication route B do not protrude beyond the width of the vascules (**Fig. 1(b)**), so it is expected that the termination of load bearing fibres caused the drop in load as the crack tip approached these vascules. Vascules formed via fabrication route A led to significant crack arrest, as seen by the sharp load increases. In the example provided, the load increased at the first vascule until it was sufficient for crack propagation; at this point the crack jumped 20mm until it arrested at the third vascule. Here, the load increased again until it was sufficient to overcome the vascule boundary and rapid 'unzipping' occurred, leading to total failure of the specimen. These findings are in line with those of Kousourakis, Mouritz and Bannister [19]. On propagation from a vascule, the crack plane is exposed to an instantaneous increase in displacement rate over the 2 mm/min set rate. Previous studies have shown the rate dependency of FRP laminates, with severe reductions in Mode I fracture toughness reported at high strain rates [26,27]. This type of uncontrolled rapid fracture is undesirable in the aerospace industry, however, the long periods of

crack arrest potentially provide time for migration and gelation of released healing agents.

For configuration TB, moderate crack arrest was seen at the vascules. Here, the stress concentrations expected at the corner resin pockets caused the vascule boundary to fail at lower strain energies versus configuration TA. The strain energy stored due to crack arrest at each vascule was insufficient to cause rapid 'unzipping' of the specimens, with the crack being arrested at each subsequent vascule (if it jumped that far). Each 'saw tooth' is indicative of the position of the vasculature in these specimens. This controlled fracture process is desirable as it suggests that, in the event of overloading, sudden rapid 'unzipping' of a component will be avoided.

Optical micrographs of the crack propagation routes are displayed in **Fig. 6**. For fabrication route A, fracture of the resin pockets ensured the crack remained between the central plies, whereas for fabrication route B the crack jumped to the corner of the effective defect (at the resin rich pocket) on progression from the first, or in some instances the second vascule. These observations confirm that Mode I propagating cracks interact with the vascules in such a way that healing agent release would be expected.

Typical load-displacement curves for aligned vascules are provided in **Fig. 7**. For both fabrication routes, the load followed that of the control sample until arrival of the crack tip at the ends of the two vascules embedded in each specimen. The rate of load decrease is reduced from this point compared to the control. The inclusion of two 0.5mm diameter vascules reduces the effective fracture plane width from 20 to 19mm, so a drop in load bearing ability could be

expected, contradictory to the experimental findings. Existing literature shows that the total energy release rate may increase substantially for curved crack fronts, compared to straight crack fronts assumed in classical beam theory [28]. It is hypothesised that the inclusion of the aligned vascules segregates the crack front, creating additional edge effects which slow crack propagation (via the same mechanisms that slow the edges of the crack front in a standard DCB test).

A summary of the average crack propagation speeds, over the portion of the DCB specimens containing vascules, are provided in **Table 1**. Configuration TA led to significant crack arrest and subsequent rapid unzipping of the test specimens, which ultimately caused faster crack propagation rates (approximately 33%) compared to the control laminate. Crack arrest occurred at each vascule along the fracture plane of configuration TB, resulting in a controlled failure of the specimen and slower propagation rates versus the control (approximately +9%). For parallel vascules, both fabrications routes appeared to slow down crack propagation by approximately 9%.

Based on the results generated, combined with experimental observations, it can be concluded that the inclusion of open vasculature does not have a detrimental effect on the fracture toughness of a unidirectional laminate subjected to a Mode I opening displacement.

4.2 Mode II crack-vascule interactions

Mode II crack propagation was found to be less stable compared to that witnessed for Mode I testing, with regions of stick-slip crack progression seen

within the control sample, particularly during the initial 20mm of crack growth. Crack propagation was found to be very similar (both visually and from force-displacement curves) for the control and the laminates containing vascules orientated parallel to the fibre direction. Edge effects are not an issue for Mode II testing, eliminating contributions from free edges at the vascules, allowing the crack to propagate with a straight front. For this reason, the crack progresses along the aligned vascules as it does for the control.

For the transverse orientated vascules, the force versus displacement curves followed very similar trends to the Mode I testing (**Fig. 5**). With fabrication route A, the crack was arrested at the first vascule followed by rapid unzipping of the remaining 20mm of the crack plane. The Mode II fracture toughness has also been reported to be rate dependent with reduced toughness recorded at high strain rates [29,30]. The crack plane immediately beyond a vascule is exposed to a rapid increase in displacement rate on crack propagation from the vascule, so uncontrolled rapid crack propagation could be expected. For fabrication route B, slight crack arrest was seen at each vascule.

Of particular interest were the crack propagation routes identified by optical microscopy, **Fig. 8**. The crack arrested at the tip of the resin rich pocket (fabrication route A), then jumped a ply interface leading to rapid unzipping of the specimen. The crack propagation route followed the fibre waviness around the vascules, in contrast to the route seen for Mode I. The propagation route for fabrication route B followed that identified for Mode I; the crack was arrested by the vascule, via crack blunting, before the strain concentration at the corner resin pockets result in a propagation route that cleaves open the subsequent

vascules. These observations have obvious implications for multifunctional composites, with fabrication route A being more suited to embedded vascularity not seeking crack interaction e.g. thermal management applications and fabrication route B more suited to those which are incumbent on crack interaction e.g. self-healing.

Similar vascules were incorporated into a 16-ply quasi-isotropic carbon fibre reinforced epoxy laminate, where the interactions of the embedded vascules with an impact event were characterised [18]. It can be seen in **Fig. 9** that the delaminations followed similar paths to those identified with the Mode II ELS testing. This suggests that the delamination formation is a Mode II driven mechanism and, therefore, the Mode II ELS test is more suited to characterisation of such vasculature than the Mode I DCB test.

Reliable, comparative crack propagation speeds could not be obtained from the Mode II evaluation as the results yielded large variations. In addition, some of the TA specimens held the crack at the first vascule throughout the test duration.

4.3 Fracture toughness

The Mode I and II maximum fracture toughness for each of the vascule configurations, along with the control, are displayed in **Fig. 10**. It should be noted that in the case of the transverse vascules, the fracture toughness represents the crack arrest measured at the vascule, rather than the toughness of the fracture plane as a whole.

For fabrication route A, transversely orientated vascules increase the maximum fracture toughness by 160% over the control laminate for Mode I and 80% for Mode II. These results fall in line with the facture path observations, whereby the Mode I crack is arrested for a significant period by the vascule via crack blunting. Under Mode II displacement, the crack is arrested by the tough resin pocket which ultimately causes the crack to jump an interface before propagation continues. This suggests the energy required to propagate the crack through the resin pocket is greater than is required for it to jump an interface under Mode II conditions. Trask & Bond [15] have shown that the formation of large resin pockets led to resin deficient zones and voids in the vicinity of vascule type TA. This is a likely contributor to the crack redirection seen in Fig 8(a). For configuration TB, a moderate increase in fracture toughness for Mode I (+32%) is seen, whereas for Mode II there is no statistical increase over the control (+6%) even though slight crack arrest was witnessed visually. For both modes, crack arrest was via a crack blunting mechanism.

Embedding vascules parallel to the fibre direction did not significantly alter the toughness of the fracture plane compared to the control, under either mode. For the Mode II fracture toughness calculations, the flexural modulus of a standard laminate was utilised in all cases. However, it is anticipated that the inclusion of the vascules will result in a slight decrease in laminate stiffness [18]. Based on equation (2), lowering the flexural modulus will lead to an increase in calculated Mode II fracture toughness, therefore, the values presented here can be regarded as conservative. Statistically, it can be concluded that the

incorporation of bioinspired vascules did not adversely affect the fracture toughness of the host laminate under Mode I and II displacements.

5. Further studies

This study has addressed a number of issues regarding the interactions of embedded vasculature and propagating cracks. However, to fully optimise and predict how such features would perform within a real-life structure, the authors suggest evaluating the following:

- *Crack propagation along 0/45° interfaces* – The use of self-healing is intended for damage tolerant laminates which typically contain 0/45° interfaces to minimise the stiffness mismatch between plies [1-3]. Therefore, it would seem prudent to evaluate the interactions of propagating cracks and vascules along such ply interfaces. However, fracture in multiaxial laminates has been shown to be considerably more complex compared to that of unidirectional Mode I or II tests [31].
- *Mixed mode properties* – It is widely accepted that damage formation under impact loading is a mixed Mode I/II process [1-3]. Therefore, the findings of this study do not truly represent that found in operationally induced damage. For laminate TA, it is anticipated that a number of tests would be required to find the ratio of Mode I/II at which there is a transition from crack propagation through to crack propagation around the resin pocket.
- *Vascule diameter and spacing* – Under Mode I displacement, it has been shown that variations in spacing for configuration TA have minimal

impact on the Mode I fracture toughness but this parameter is sensitive to vascule diameter [19]. The effects of these parameters are yet to be determined for the other configurations evaluated in this study for Mode I, and all configurations for Mode II. It is anticipated that there will be some compromise with the vascule size and spacing that offers the greatest potential for effective self-healing and the most desirable fracture characteristics.

- *Fatigue properties* – The growth of delaminations under cyclic loading can lead to catastrophic failure in much the same way as under static loading. Therefore, evaluating the interactions of vasculature and fatigue cracks would be of significant interest.
- *Manipulation of the crack-vascule interactions* – In the context of the CRASHCOMPS project, where the goal is to manipulate cracks and redirect them to regions of self-healing, the crack propagation direction needs to be predictable. Ideally, features can be incorporated within the laminate, in the vicinity of the vascules, to manipulate the crack front and rate of propagation, in order to maximise self-healing effectiveness.
- *Z-pins to inhibit unstable crack growth* – The utilisation of Z-pins has been shown to stop unstable crack growth under Mode I conditions [32]. The reinforcement offered by Z-pins may, therefore, offer a route to controlling crack propagation adjacent to the vascules [33,34].

6. Conclusions

Embedded bioinspired vasculature was successfully incorporated into a glass fibre reinforced epoxy laminate, using 0.5mm diameter steel wire as the vascule preform material. The wire was either laid between plies (fabrication route A) or nested in pre-cut recesses within the plies (fabrication route B) during the stacking sequence. The vascule fabrication route adopted played a significant role on the laminate morphology which in-turn dictated the crack-vascule interactions.

Transversely orientated vascules embedding via fabrication route A led to the formation of large resin pockets on the front and back faces along with significant fibre waviness. Under Mode I opening, the resin pocket fractured ensuring the crack was arrested by the vascule through a blunting mechanism. Under Mode II displacement, the resin pocket itself arrested the crack until the stored strain energy was sufficient for the crack to jump a ply interface and follow the fibre waviness around the vascule. In both cases, significant crack arrest was observed which lead to rapid ‘unzipping’ of the fracture plane beyond the vascule location.

Transversely orientated vascules embedded via fabrication route B, led to small corner resin pockets from the embedment of a circular preform into a square recess. This morphology ensured crack-vascule interactions under Mode I and II displacements and is, therefore, deemed more suited to an application requiring reliable crack interaction e.g. self-healing. Crack arrest for both modes was significantly lower compared to the transverse fabrication route A vascules, leading to controlled failure of the fracture plane.

When aligning the vascules to the fibre direction, the fibres 'fit' naturally around the inclusion, eliminating resin pockets and fibre waviness. Aligned vascules did not significantly affect the Mode I and II fracture toughness. It can be concluded that statistically, none of the vascule configurations evaluated lowered the Mode I or II fracture toughness of the host laminate.

Acknowledgements

The authors would like to thank the UK Engineering and Physical Sciences Research Council and UK Ministry of Defence via Defence Science and Technology Laboratory for funding this work under CRASHCOMPS (EP/G003599), Airbus UK for their additional financial support and Amir Rezai and David Fishpool at BAE Systems for their assistance with the Mode II ELS testing.

References

[1] Cantwell WJ, Morton J. The impact resistance of composite materials - a review. Composites 1991;22:347-62.
[2] Hull D, Shi YB. Damage mechanism characterization in composite damage tolerance investigations. Compo Struct 1993;23:99-120.
[3] Richardson MOW, Wisheart. Review of low-velocity impact properties of composite materials. Composites A 1996;27:1123-31.
[4] Williams HR, Trask RS, Weaver PM, Bond IP. Minimum mass vascular networks in multifunctional materials. J R Soc Interface 2008;5:55-65.
[5] Kessler MR, White SR. Self-activated healing of delamination damage in woven composites. Composites A 2001;32:683-99.
[6] White SR, Sottos NR, Moore J, Geubelle P, Kessler M, Brown E, et al. Autonomic healing of polymer composites. Nature 2001;409:794-7.
[7] Patel AJ, Sottos NR, Wetzel ED, White SR. Autonomic healing of low-velocity impact damage in fiber-reinforced composites. Composites A 2009;41:360-8.
[8] Trask RS, Bond IP. Biomimetic self-healing of advanced composite structures using hollow glass fibres. Smart Mater Struct 2006;15:704-10.
[9] Williams GJ, Trask RS, Bond IP. A self-healing carbon fibre reinforced polymer for aerospace applications. Composites A 2007;38:1525-32.
[10] Williams GJ, Bond IP, Trask RS. Compression after impact assessment of self-healing CFRP. Composites A 2009;40:1399-406.
[11] Toohey KS, Sottos NR, Lewis JA, Moore JS, White SR. Self-healing materials with microvascular networks. Nat Mater 2007;6:581-5.

[12] Toohey KS, Hansen CJ, Lewis JA, White SR, Sottos NR. Delivery of two-part self-healing chemistry via microvascular networks. Adv Funct Mater 2009;19:1399-405.
[13] Williams HR, Trask RS, Bond IP. Self-healing composite sandwich structures. Smart Mater Struct 2007;16:1198-207.
[14] Williams HR, Trask RS, Bond IP. Self-healing sandwich panels: restoration of compressive strength after impact. Compos Sci Technol 2008;68:3171-77.
[15] Trask RS, Bond IP. Bioinspired engineering study of plantae vascules for self-healing composite structures. J R Soc Interface 2010;7:921-31.
[16] Huang C-Y, Trask RS, Bond IP. Characterization and analysis of carbon fibre-reinforced polymer composite laminates with embedded circular vasculature. J R Soc Interface 2010;7:1229-41.
[17] Kousourakis A, Bannister MK, Mouritz AP. Tensile and compressive properties of polymer laminates containing internal sensor cavities. Composites A 2008;39:1394-403.
[18] Norris CJ, Trask RS, Bond IP. The role of embedded bioinspired vasculature on damage formation in self-healing carbon fibre reinforced composites. Composites A; Accepted for publication, January 2011.
[19] Kousourakis A, Mouritz AP, Bannister MK. Interlaminar properties of polymer laminates containing internal sensor cavities. Compo Struct 2006;75:610-18.
[20] ASTM International Mode I Interlaminar fracture toughness of unidirectional fiber-reinforced polymer matrix composites, test method designation: D5528.
[21] Wang H, Vu-Khanh T. Use of end-loaded-split (ELS) test to study stable fracture behaviour of composites under mode II loading. Compo Struct 1996;36:71-9.
[22] Blackman BRK, Brunner AJ, Williams JG. Mode II fracture testing of composites: a new look at an old problem. Engineering Fracture Mechanics 2006;73:2443-55.
[23] Wang WX, Nakata M, Takao Y, Matsubara T. Experimental investigation on test methods for mode II interlaminar fracture testing of carbon fiber reinforced composites. Composites A 2009;40:1447-55.
[24] European Structural & Integrity Society, Technical Committee 4 (ESIS-TC4). Fibre-reinforced plastic composites – determination of apparent Mode II interlaminar fracture toughness, G IIc, for unidirectionally reinforced materials. Version 01-04-02.
[25] Williams JG. On the calculation of energy release rates for cracked laminates. Int J Fracture 1988;36:101-19.
[26] Smiley AJ, Pipes RB. Rate effects on Mode I interlaminar fracture toughness in composite materials. J Compos Mater 1987;21:670-87.
[27] Kusaka T, Hojo M, Mai YW, Kurokawa T, Nojima T, Ochiai S. Rate dependence of Mode I fracture behaviour in carbon-fibre/epoxy composite laminates. Compos Sci Technol 1998;58:591-602.
[28] Nilsson K-F. On growth of crack fronts in the DCB-test. Compos Eng 1993;3:527-46.
[29] Smiley AJ, Pipes RB. Rate sensitivity of Mode II interlaminar fracture toughness in graphite/epoxy and graphite/PEEK composite materials. Compos Sci Technol 1987;29:1-15.
[30] Kusaka T, Hojo M, Ochiai S, Kurokawa T. Rate-dependent mode II interlaminar fracture behaviour of carbon-fiber/epoxy composite laminates. Mater Sci Res Int 1999;5:98-103.
[31] Choi NS, Kinloch AJ, Williams JG. Carbon-fiber/epoxy composites under Mode I, Mode II and mixed-mode I/II loading. J Compos Mater 1999;33:73-100.
[32] Cartié DDR, Cox BN, Fleck BN. Mechanisms of crack bridging by composite and metallic rods. Composites A 2004;35:1325–36.
[33] Mouritz AP. Review of Z-pinned composite laminates. Composites A 2007;38:2383-97.
[34] Mouritz AP, Cox BN. A mechanistic interpretation of the comparative in-plane mechanical properties of 3D woven, stitched and pinned composites. Composites A 2010;41:709-28.

Table 1. Average crack propagation speed from where the crack meets the 1st vascule until the test was ended.

	Control	Transverse Fab. A	Transverse Fab. B	Parallel Fab. A	Parallel Fab. B
Propagation rate post 1st vascule, μm/s	46 (± 1)	60 (± 5)	42 (± 3)	42 (± 3)	42 (± 2)

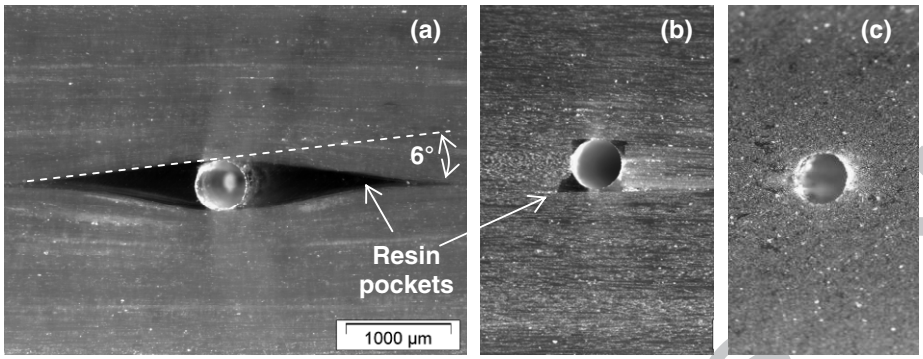

Fig. 1. Vascule characterisation; (a) transverse fabrication route A, (b) transverse fabrication route B and (c) aligned vascule representative of both fabrication routes.

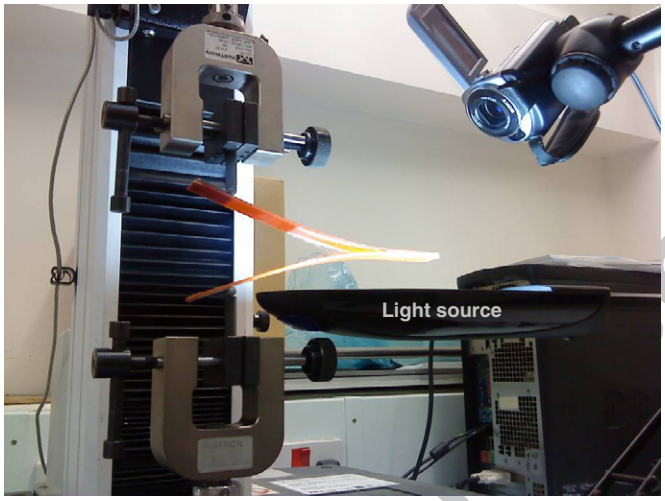

Fig. 2. Mode I DCB crack monitoring.

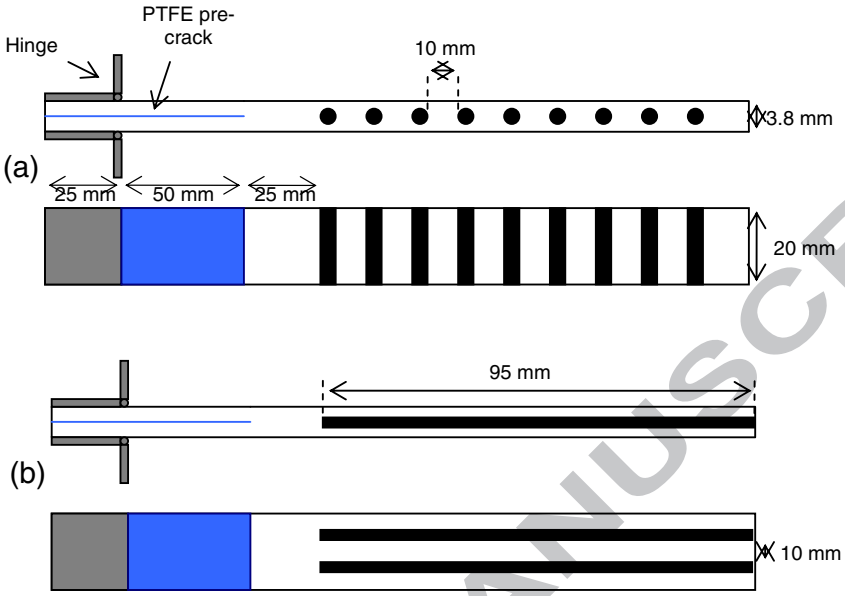

Fig. 3. Mode I DCB specimen geometry; (a) transverse vascules and (b) aligned vascules.

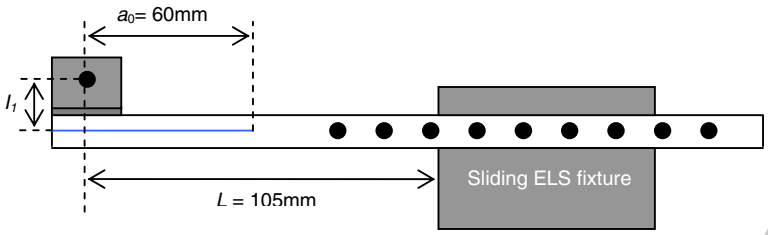

Fig. 4. Mode II ELS specimen geometry.

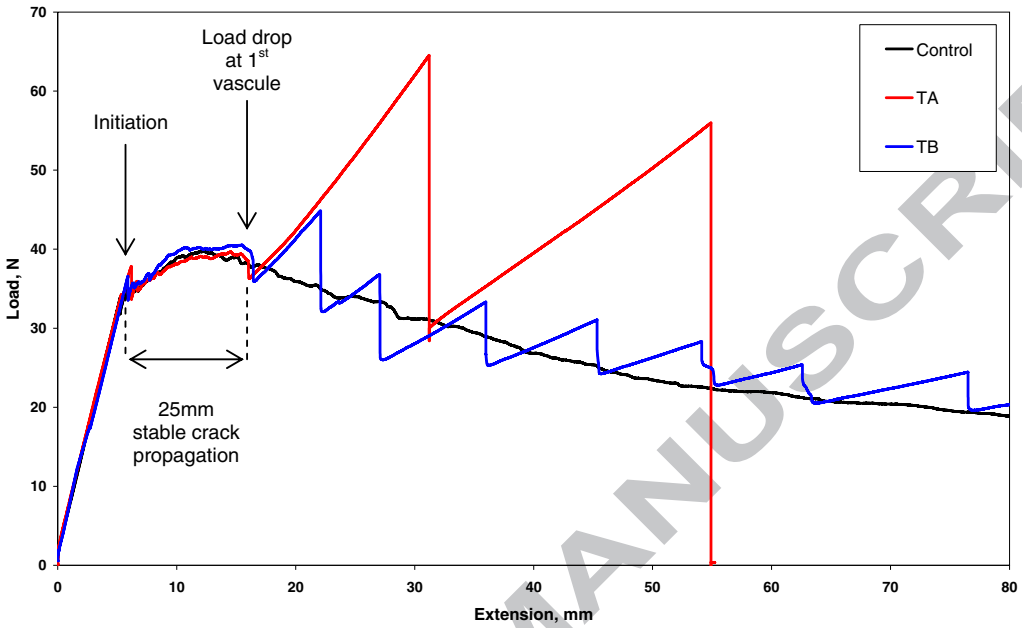

Fig. 5. Mode I load vs. displacement curves for transverse orientated vascules (T= transverse, A = fabrication route A and B = fabrication route B).

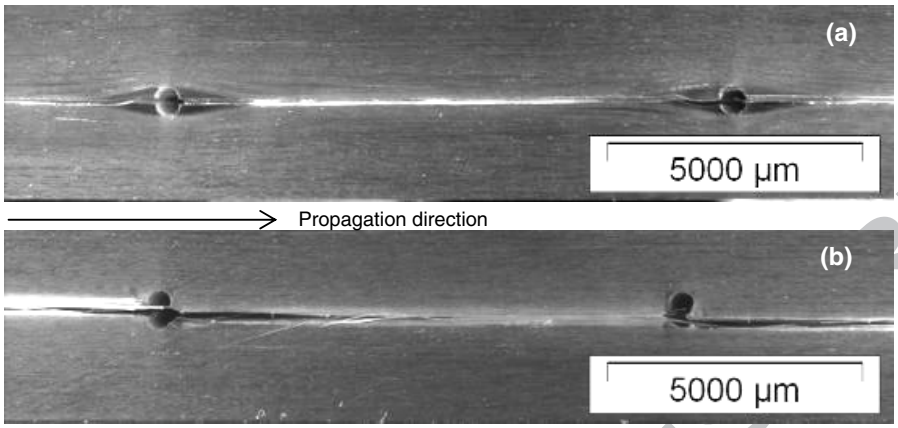

Fig. 6. Mode I crack propagation routes; (a) transverse fabrication route A, (b) transverse fabrication route B.

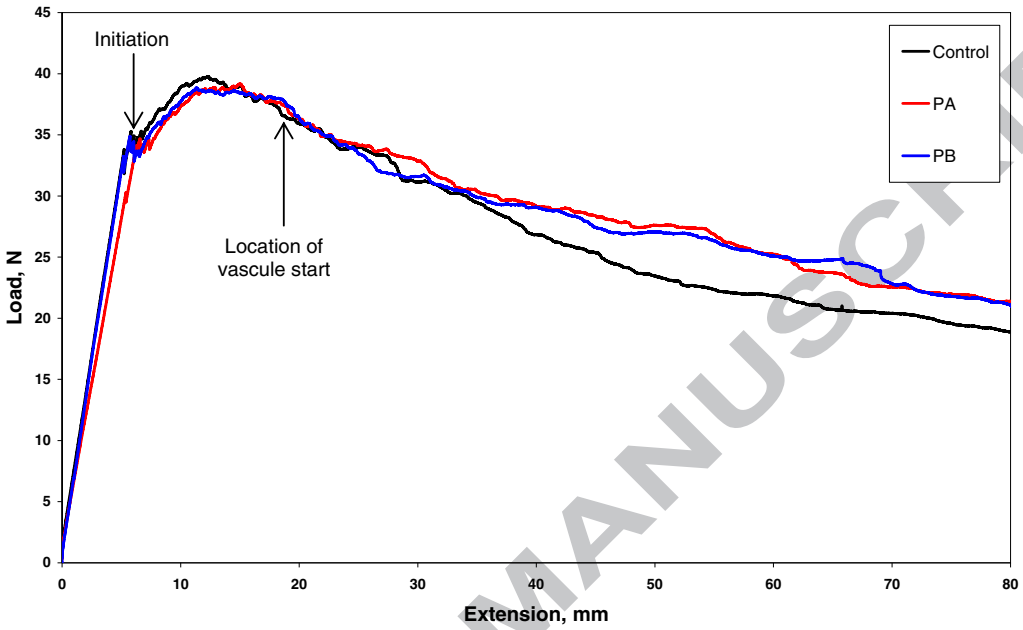

Fig. 7. Mode I load vs. displacement curves for vascules aligned parallel to the fibre direction (P = parallel, A = fabrication route A and B = fabrication route B).

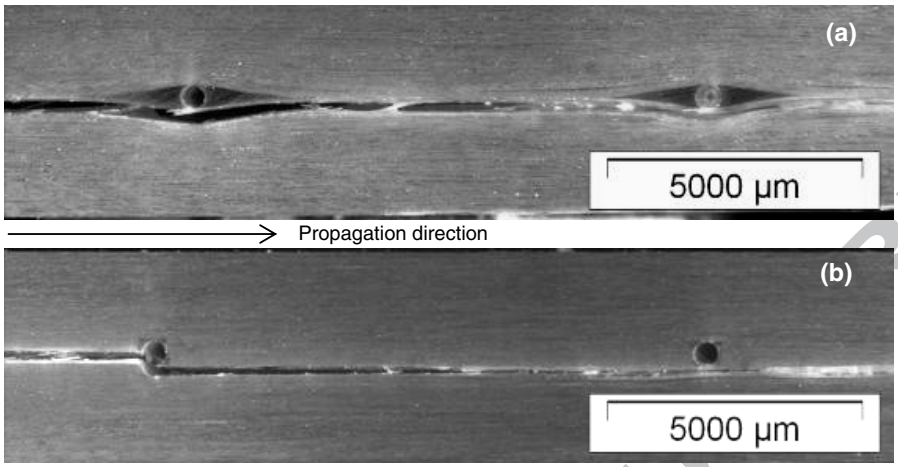

Fig. 8. Mode II crack propagation routes; (a) transverse fabrication route A, (b) transverse fabrication route B.

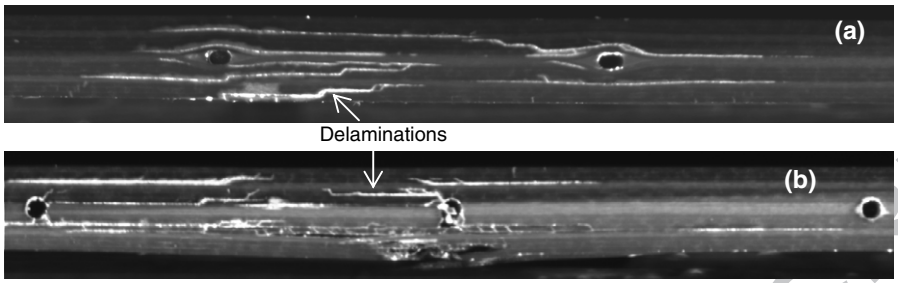

Fig. 9. Impact delamination routes; (a) transverse fabrication route A, (b) transverse fabrication route B.

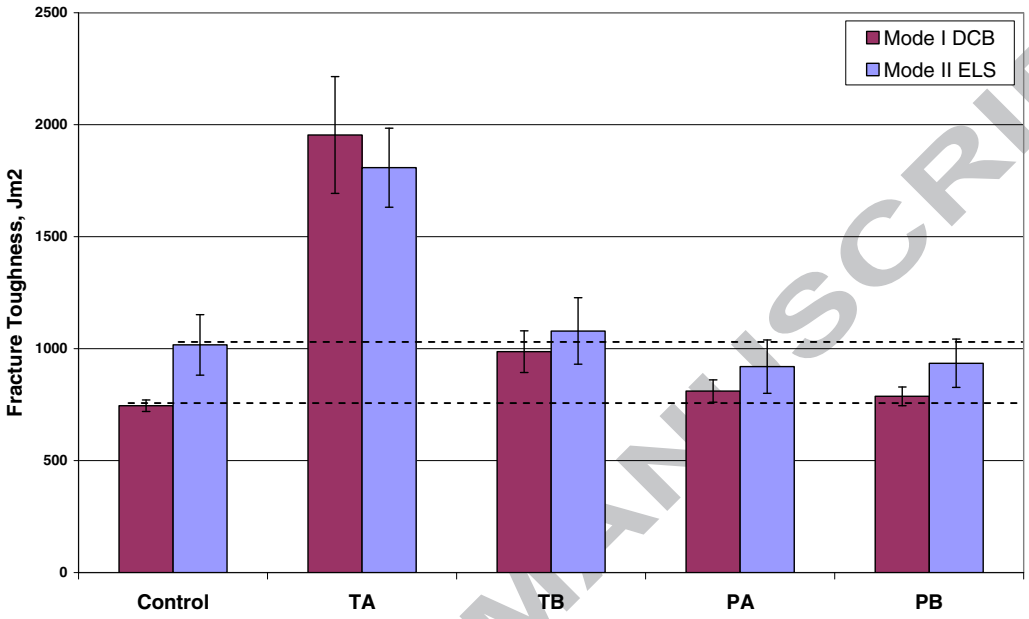

Fig. 10. Mode I and Mode II fracture toughness.